Summary after lecture 8th

8th Data Analysis:

Archives, catalogs and software:

- **mission dependent**
- **mission independent**
- **deep sky survey**

Calibration data:

- **imaging-analysis**
- **spectral-analysis**
- **timing-analysis**

Spectral fitting:

- **RMF, ARF**
- **forward fitting**

Models in fitting softwares:

- **additive**
- **multiplicative**

General considerations on fitting:

- **minimization**
- **bkgr fitting**
- **source detection algorithm**

Timing analysis:

Lecture 9: Extended sources

The process requires to isolate the source from the bkgr. PSPC and CCDs combine spectra with imaging, and this requires more complex procedures, simultaneous analysis of both the spectra and the photometry:

Detectors are not ideal, therefore:

- if the source is not large compared to the PSF, then the flux in the source region must be corrected for flux falling outside the region (important for large PSF like on SUZAKU)
- instrumental response may vary significantly over the source region,
- the variation between source and background regions will be even greater.

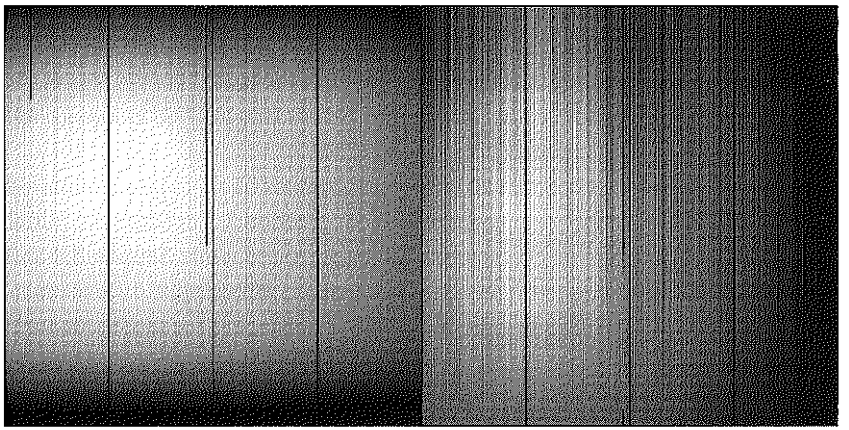

Fig. 8.1 [Left] The Chandra effective area at 1.0 keV as a function of position on the S3 chip. [Right] The Chandra effective area at 6.0 keV as a function of position on the S3 chip. Both images have been stretched from 80% to 100% of the maximum response

Backgrounds and foregrounds:

Instrumental bkgr: particles interact with detector:

1) The particle background – recorded by the instrument when it is not exposed to cosmic X-rays.

I.e. ASCA, and SUZAKU observed the night side of the Earth other satellites on "stowed position". CHANDRA

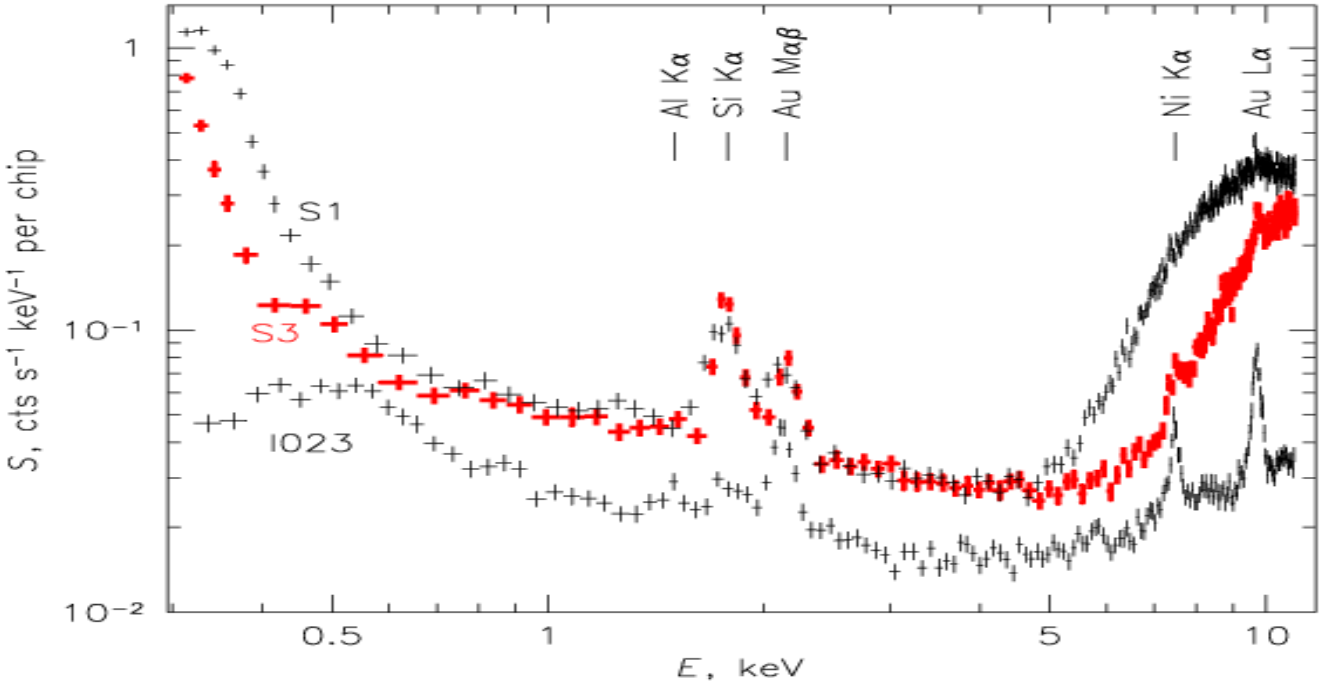

Backgrounds and foregrounds:

Continuum – from direct interaction of the particles with the detector.

Lines – due to fluorescence of the surrounding material.

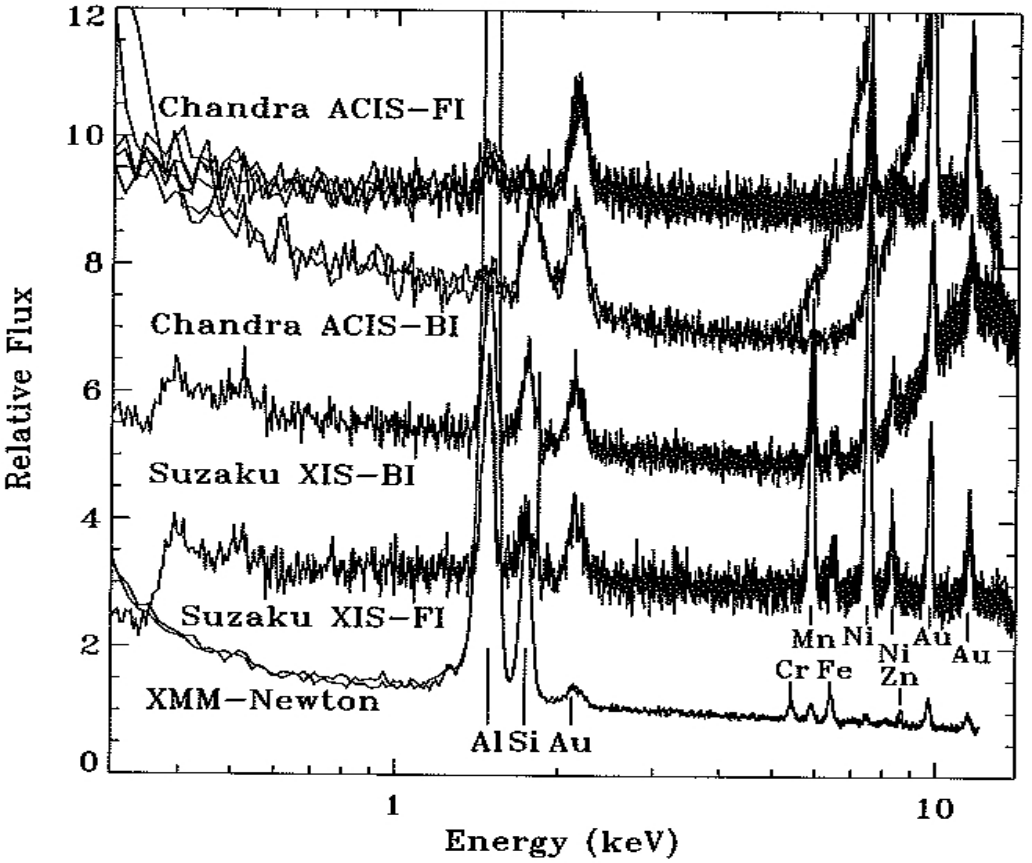

Fig. 8.2 Typical particle background spectra from current missions. Prominent lines are identified. Curves have been normalized and offset for clarity. *FI:* Front-side illuminated; *BI:* back-side illuminated

The particle bkgr varies with time, stays significant with energy. "Blank Sky" Standard particle bkgr spectra are available for modern missions.

Backgrounds and foregrounds:

2) The soft-proton contamination (SPC) - one of the unpleasant surprises of the Chandra and XMM-Newton missions was that the mirrors focus low-energy protons (~150 keV) onto the detectors. Modulated by the Earth's magnetic field, soft-proton flux depends on time, spacecraft location, the pointing direction.

Strongly variable on timescales from seconds to hours.

Soft-proton vignetting (distribution over the detector) is different from the photon vignetting.

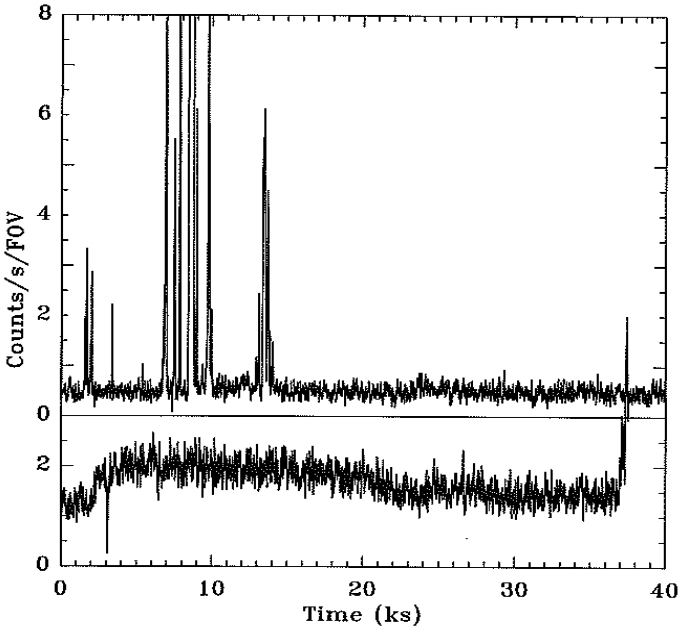

Fig. 8.3 Lightcurves showing soft-proton contamination in XMM–Newton observations. The top plot is a typical lightcurve; the soft-proton contributions are strong but of limited duration. The bottom plot shows that the soft-proton contribution can be relatively constant for an extended period of time; a flat lightcurve for a short (10 ks) observation is no guarantee of low soft-proton contamination

Backgrounds and foregrounds:

Cosmic background: diffuse X-ray bkgr, Galactic emission, heliospheric emission, Earth's emission.

1) The extragalactic bkgr: in the 0.1-10.0 keV band it is composed almost exclusively by unresolved AGN. If something else ????? active area of research, especially at lower energies. Typical emission of unresolved AGN can be modeled by power – law of photon index ~1.4

2) The Galactic Foreground: at least two components at high Galactic latitudes, and even more in the disk:

Local Hot Bubble (LHB) – irregular region surrounding the Sun with radius 100-200 pc $T \sim 10^6$ K.

Galactic Halo (GH) – with $T \sim 1 - 3\ 10^6$, seen in each obs.

Backgrounds and foregrounds:

LHB and GH
can be well fitted by collisional ionization models the emission is predominantly by lines and the bulk of the emission falls below 1.5 keV.

If the source has big flux below 1.5 keV then the Galactic foreground must be treated with caution. Best fit with APEC or MEKAL models.

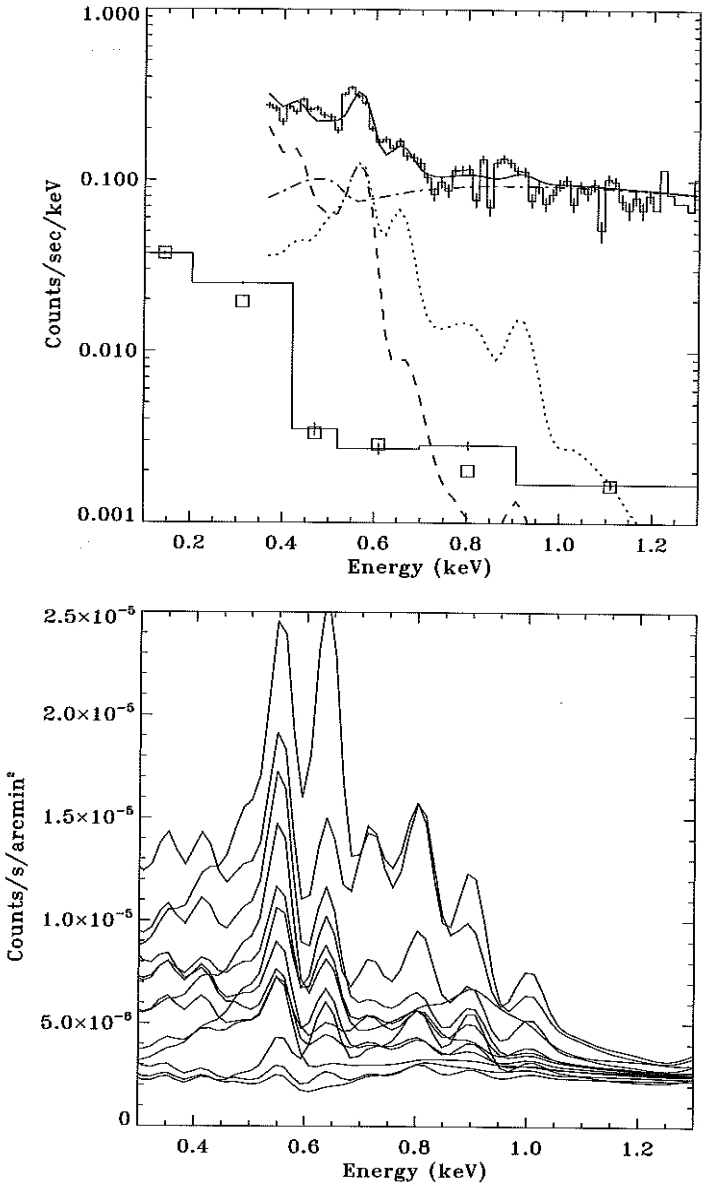

Fig. 8.4 [Top] Typical high Galactic latitude spectrum, taken with XMM–Newton, decomposed into LHB (dashed), halo (dotted), and background AGN (dot–dashed). The lower line (data) with boxes (model) is the RASS spectrum for the same region. [Bottom] The variety of Galactic foreground spectra

Backgrounds and foregrounds:

3) Heliospheric and geocoronal emission:

solar wind contains ions which emit x-rays when they interact with neutral H nand He and exchange an electron.

Unknown till ROSAT.

Solar-wind charge exchange (SWCX) emission produced by interaction of the solar wind with the neutral interstellar medium.

Observed by ROSAT as on hour to week variable *"long-term enhancements"*.

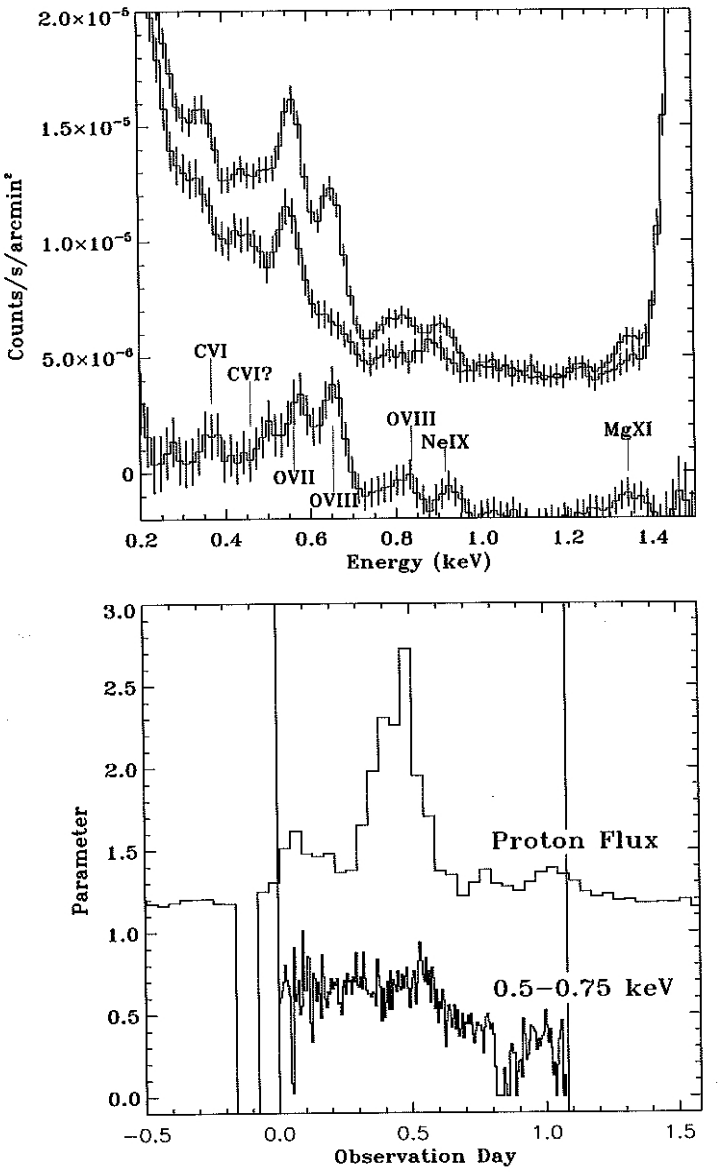

Fig. 8.5 [Top] Two different XMM–Newton observations of the same field (in this case the HST Deep Field), showing the variability of the SWCX contamination. The bottom line is the difference offset by -2.0×10^{-6}. [Bottom] The ACE proton data (top) and the 0.5–0.75 keV lightcurve for the observation interval more strongly contaminated by SWCX emission. The difference in the curves is due to geometric effects

Backgrounds and foregrounds:

Heliospheric emission is still poorly understood.

4) Exospheric emission: spacecraft with low Earth orbit (SUZAKU) often observe close to the limb of the Earth.
Be careful on aurorae and solar X-ray scattered from the Earth's atmosphere.

Backgrounds and foregrounds:

For any observation of extended emission:

- always remove particle bkgr
- Chandra XMM-Newton always have some soft-proton contamination
- ROSAT and SUZAKU exospheric contamination
- importance of extragalactic bkgr, Galactic foreground and SWCX depends on the location and spectral shape of the object.
- RASS (ROSAT All Sky Survey) count rates and simple models of the Galactic foreground to estimate the extend of the problem to your object.

Initial analysis:

1) *Lightcurves*: To determine the extend of the contamination by time-dependent bkgr it is best to create lightcurves for the emission from the entire FOV, excluding any bright variable sources.

2) *Point-source removal*: removing point sources usually removes a significant source of noise at only a small expense of data from the diffuse emission of interest.

3) *Spectral analysis*: setting the source and bkgr regions is a question of scientific need and personal taste; extracting the spectra from those regions, a question of preferred analysis package; and spectral fitting, a question of experience.

Only bkgr which can be directly subtracted from the observed spectra is the particle bkgr, the other bkgrs must be modeled.

Image analysis:

The image analysis should always be shaped by an understanding of the source and bkgr spectra. The broader the bandpass, the more difficult the bkgr removal and subsequent analysis.

1) Building the right effective area map: in the most general analysis, the fluxed image (counts/cm^2/s/pixel) is created by dividing a raw image (counts/pixel) by the EA(cm^2) and the exposure time. EA(i, j, E) is equivalent of a flat-field or instrument response map, and is function of the pixel position (i, j) and energy, E. Monochromatic EA map usually emission weighted:

$$R(i,j) = \sum_E EA(i,j,E)S(E) / \sum_E S(E)$$

where S(E) emission over the bandpass.

Image analysis:

2) Building bkgr maps from bkgr spectra: since bkgr components have different spectral shape and different distribution across a detector, it is usually a good idea to remove all bkgr before dividing the raw image by the EA map. At the very least, the particle bkgr PB(i,j) and the soft-proton image SP(i,j) should be subtracted. If $R_b(i,j)$ is the EA map created from/for the bkgr spectrum, $S_b(E)$, then the bkgr image is:

$$C_b(i,j) = R_b(i,j) \sum_E S_b(E)\, t$$

where t is exposure time.

Image analysis:

3) Subtracting the bkgr: all components from raw-count image I(i,j).

$$C_s(i,j) = \frac{1}{R_S(i,j)\,t}\left[I(i,j) - PB(i,j) - SP(i,j) - \sum_N \left[R_n(i,j) \sum_E S_n(E)\,t \right] \right]$$

EA for the source spectrum

raw image

particle bkgr

soft-proton bkgr

sum over all X-ray bkgr Gal. foreground, extragalactic bkgr, exospheric emission.

Image analysis:

3) Subtracting the bkgr: all components from raw-count image I(i,j):

$$C_s(i,j) = \frac{1}{R_S(i,j)\,t}\left[I(i,j) - PB(i,j) - SP(i,j) - \sum_N \left[R_n(i,j) \sum_E S_n(E)\,t \right] \right]$$

EA for the source spectrum

raw image

particle bkgr

soft-proton bkgr

sum over all X-ray bkgr Gal. foreground, extragalactic bkgr, exospheric emission.

If the spatial variation of the response to the bkgr is very similar to the spatial variation of the response to the source:

$$C_s(i,j) = \frac{I(i,j) - PB(i,j) - SP(i,j)}{R_S(i,j)\,t} - \sum_N \left[\frac{R_n}{R_S} \sum_E S_n(E)\,t \right]$$

small differences of EA, and bkgr much fainter than source.

Image analysis:

4.) A more simple bkgr construction: assuming that spectral shape of the bkgr has been fit or it is known. Therefore the bkgr subtraction will only be good as the spectral fit. Poor spectral fit to get a roughly correct EA map and then to use the measured number of bkgr counts, B' , in some region denoted by primes, to get:

$$C_B(i,j) = \left[\frac{B'}{\sum R_B(i',j')} \right] R_B(i,j)$$

For Chandra data, an emission-weighted effective area map can be made easily using CIAO.... :)

Handbook of X-ray astronomy 2011

Statistics:

X-ray astronomers need statistics to make decisions in science, evaluate observation, models, formulate questions and proceed forward with investigations.

(Handbook for X-ray astronomy, 2011)

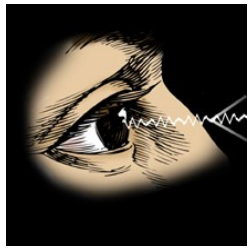

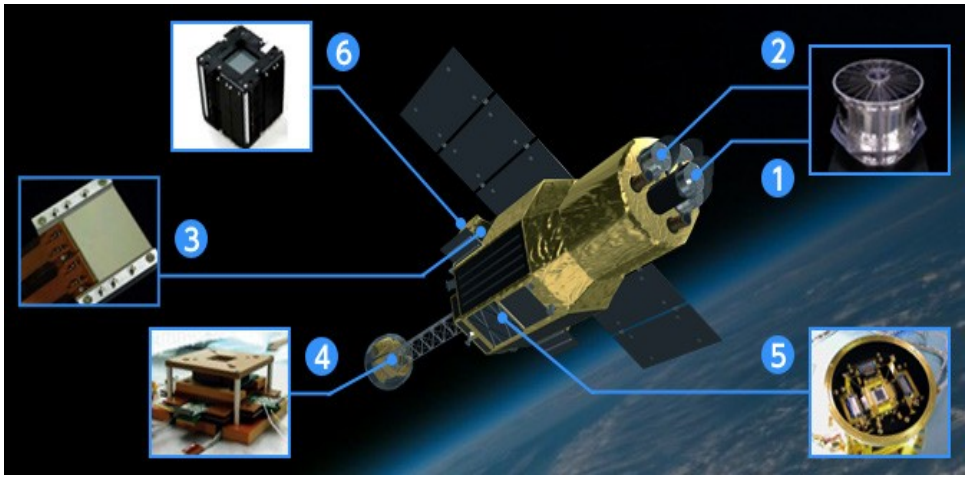

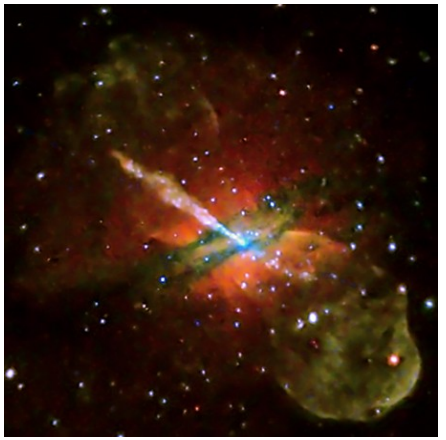

$C(PI)$ → unfolded spectrum → S_j

↑ fitting

convolution with response

theoretical model:

$B(PI)$ ← $R_{ij} A_j \times M_j$ ← M_j

"Statistics are needed at every step of scientific analysis"

OBSERVATION – experiment design, time of exposure, number of objects, type ?

REDUCTION – S/N ratio, data quality, background, algorithms, calibration files: RMF, ARF, PSF, exposure maps,

FORWARD FITTING – parameter estimation, hypothesis testing, distribution testing, correlations, etc....

$$C(PI) \approx T \sum_j R_{ij} A_j S_j \quad \leftarrow \text{Source}$$

$$B(PI) \approx T \sum_j R_{ij} A_j M_j \quad \leftarrow \text{Model}$$

Comparison to theory:

Measurements give us series of numbers: $y_i \pm \sigma_i$

If we have Poisson statistic: $\sigma_i = \sqrt{(y_i)}$

but in general: $\sigma_i \neq \sqrt{(y_i)}$

if numbers were not further processed.

Comparison to theory:

Measurements give us series of numbers: $y_i \pm \sigma_i$

If we have Poisson statistic: $\sigma_i = \sqrt{(y_i)}$

but in general: $\sigma_i \neq \sqrt{(y_i)}$

if numbers were not further processed.

Suppose we make two measurements counting meteors per night:

- 20 in one night
- 30 in second night

unprocessed obey Poisson:

$$N_1 = 20 \pm 4.47, \qquad N_2 = 30 \pm 5.58$$

Comparison to theory:

Measurements give us series of numbers: $y_i \pm \sigma_i$

If we have Poisson statistic: $\sigma_i = \sqrt{(y_i)}$

but in general: $\sigma_i \neq \sqrt{(y_i)}$

if numbers were not further processed.

Suppose we make two measurements counting meteors per night:

- 20 in one night
- 30 in second night

unprocessed obey Poisson:

$$N_1 = 20 \pm 4.47, \qquad N_2 = 30 \pm 5.58$$

Mean:

$$\bar{N} = \frac{N_1 + N_2}{2} \pm \frac{\sqrt{(\sigma_1^2 + \sigma_2^2)}}{2} = 25 \pm 3{,}53$$

Finding parameters and checking hypotheses:

The best estimate of the true value is:

$$\bar{N} = 25 \pm 3{,}53$$

uncertainty is a standard deviation of the average.
But it is uncertain since is based on normal distribution,
and of course 2 σ value is highly possible i.e. 32 or 17....

Finding parameters and checking hypotheses:

The best estimate of the true value is:

$$\bar{N} = 25 \pm 3{,}53$$

uncertainty is a standard deviation of the average.
But it is uncertain since is based on normal distribution, and of course 2 σ value is highly possible i.e. 32 or 17....

We can expect that the rate in this experiment increases, so the difference:

$$N_2 - N_1 = N_2 - N_1 \pm \sqrt{(\sigma_1^2 + \sigma_2^2)} = 10 \pm 7.07$$

If the measurement fluctuates with 2 σ deviation, this result is quite consistent with zero. The measured value is only 1.4 standard deviation from zero. Constant rate Hypothesis possible.

Least squares fit:

We make several measurements during several night:

$x_i;$ $\quad y_i \pm \sigma_i$

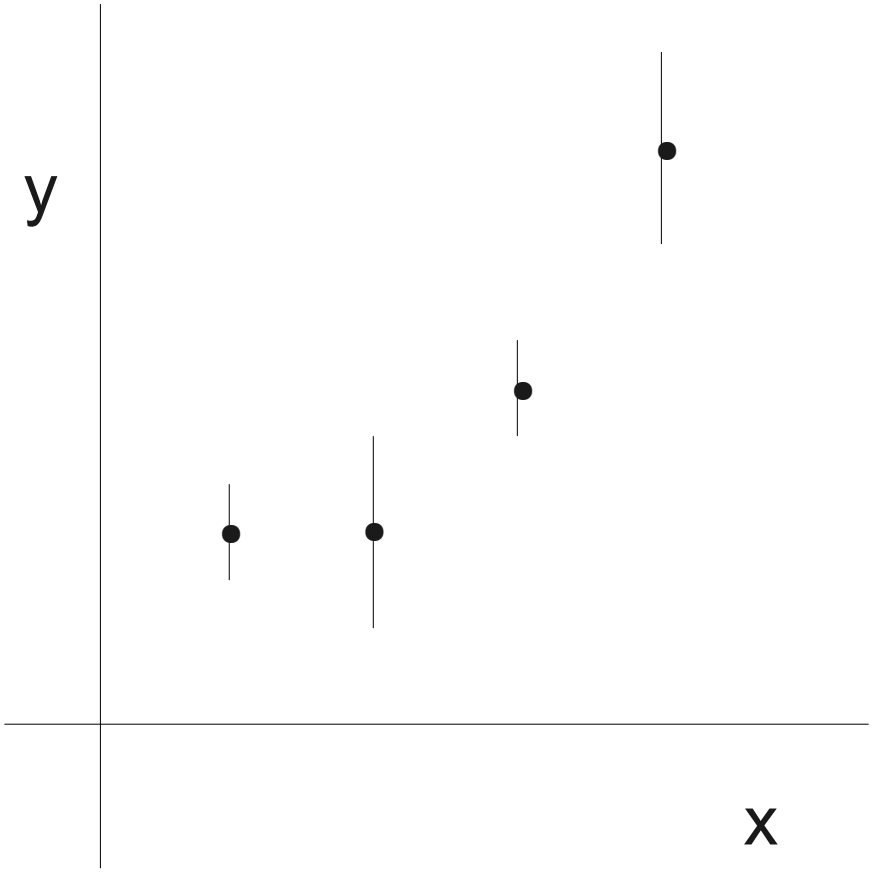

Least squares fit:

We make several measurements during several night:

$x_i;$ $\quad y_i \pm \sigma_i$

At each point we can calculate the deviation of the observed data point from the point of a theoretical curve. $y_{th,i}$

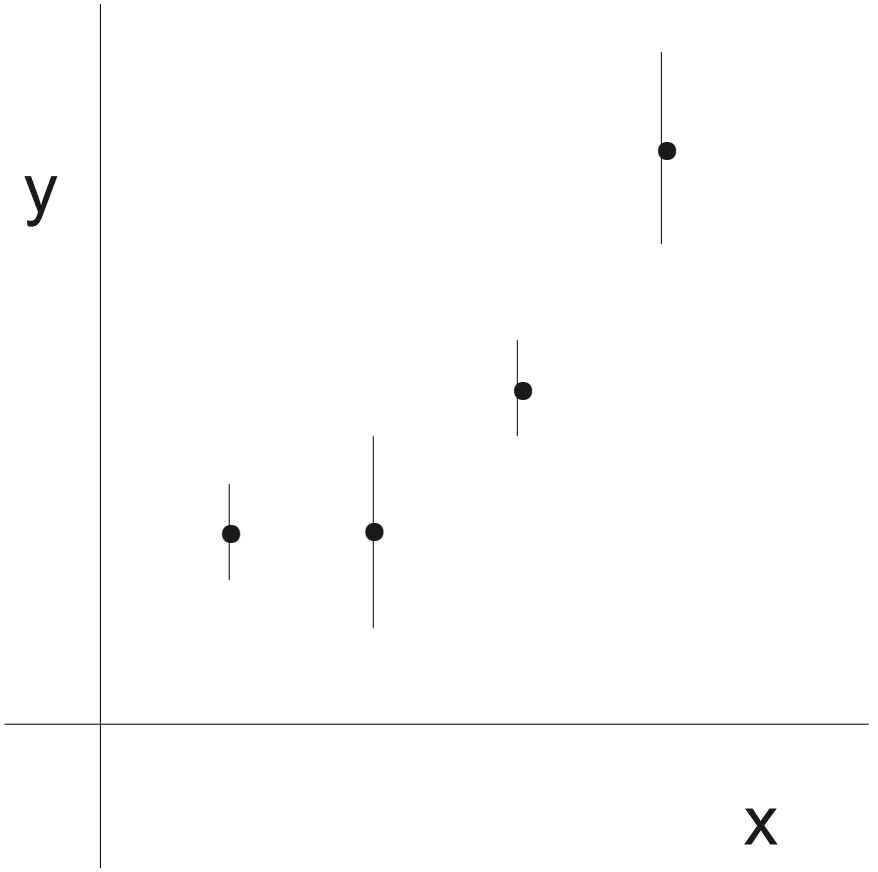

Least squares fit:

We make several measurements during several night:

$$x_i; \qquad y_i \pm \sigma_i$$

At each point we can calculate the deviation of the observed data point from the point of a theoretical curve. $y_{th,i}$
In units of standard deviation, we obtain chi square:

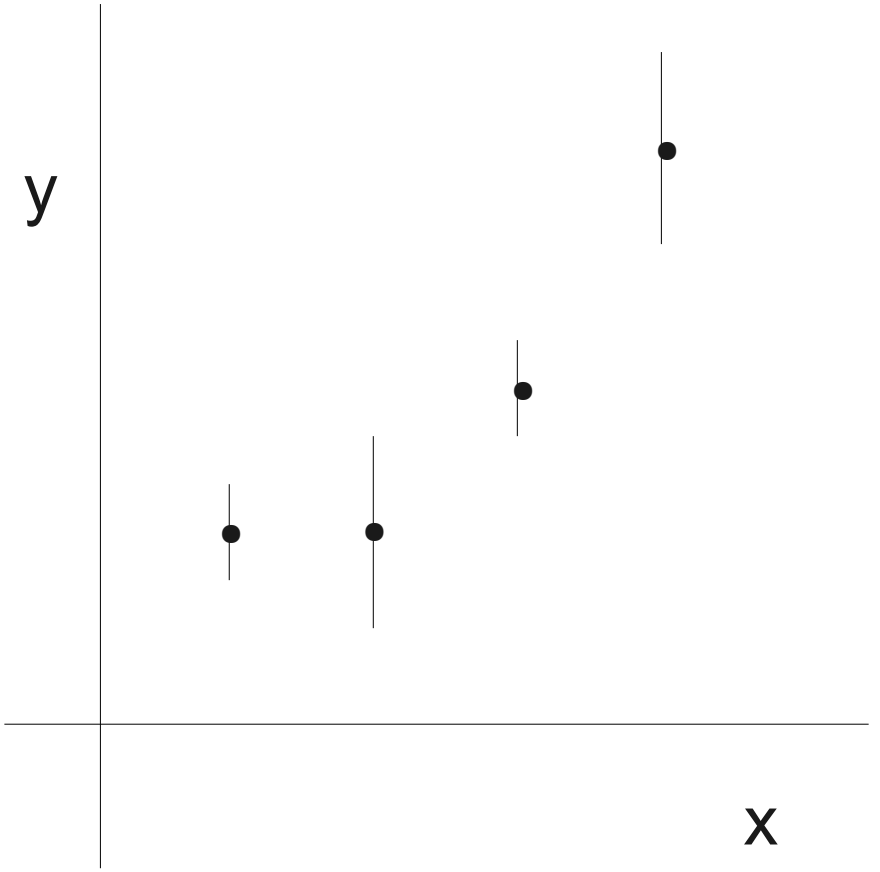

$$\chi^2 \equiv \sum_i \left[\frac{y_{ob,i} - y_{th,i}}{\sigma_i} \right]^2$$

Always positive value of the chi square, sigma calculated from the actual value of $y_{ob,i}$, since we don't know the mean.

Least squares fit:

Theoretical value of $y_{th,i}$ can be based on any function, in X-ray forward fitting on any model. The simplest is a straight line:

$$y_{th,i} = a + b\,x_i$$

line tells us if the rate of meteors per night increases, or not.
For b=0 the rate is constant in time:

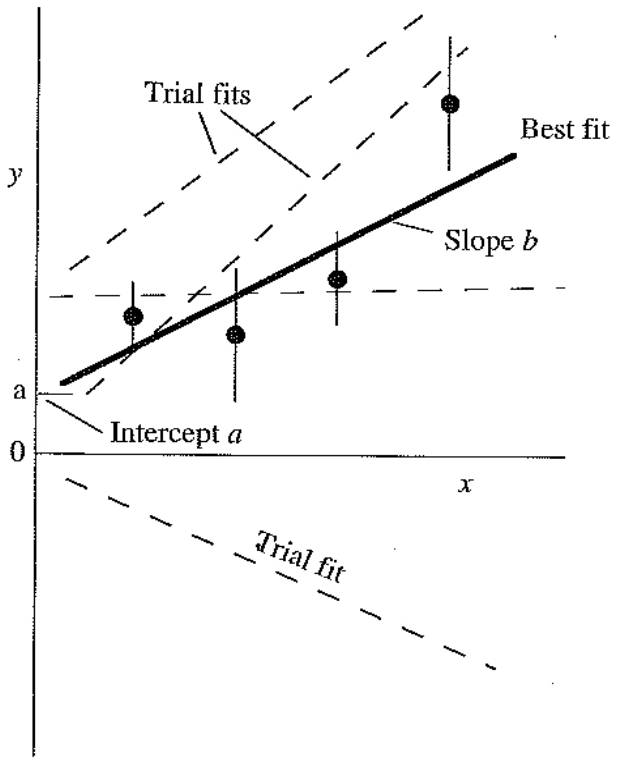

Figure 6.9. Least squares fits. The solid line is a by-eye fit to the data points in an effort to minimize χ^2 given in (21), namely the sum of the squares of the deviations, the latter being in units of the standard deviations. The dashed lines are fits that would have larger values of χ^2 and thus are less good, or terrible, fits.

Minimization – many trials of different strait lines.

Best fit value – when the minimum of chi square is obtained.

Least squares fit:

Dobrzycki + 2007

Photo-electric absorption (warm absorption):

$$M_1(E) = \exp(-N_H \sigma_{el}(E))$$

Power-law:

$$M_2(E) = A\,E^{-\gamma}$$

We fit to the observed counts C(PI):

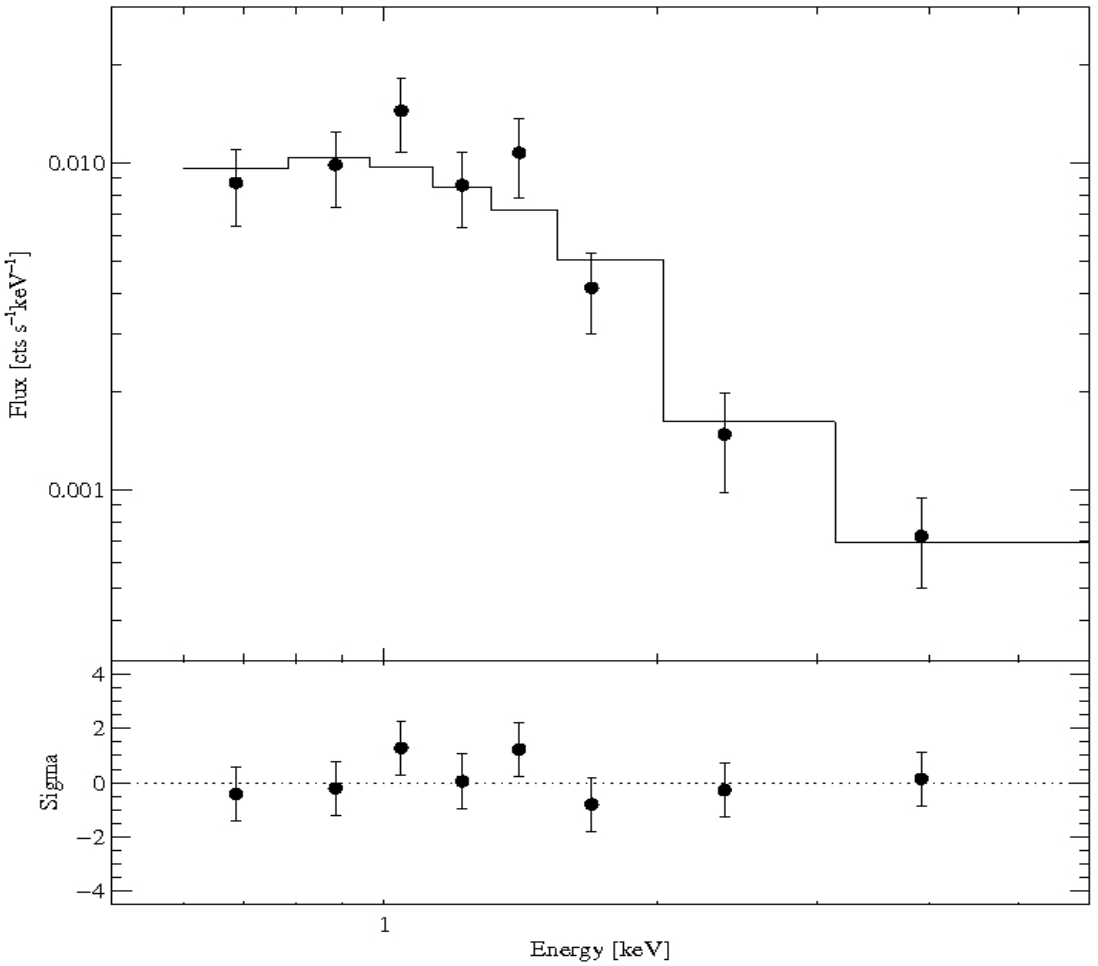

$$B(PI) \approx T \sum_j R_{ij} A_j M_{1,j} * M_{2,j}$$

Chi square test:

Is theory consistent with the data?

high chi square ⟹ to bad
low chi square ⟹ to good

The general answer is expressed in terms of probabilities, and uses directly the value of chi square calculated from the data together with the number of degrees of freedom f:

$$f = n - p$$

number of data points

number of fitted parameters

Chi square test:

$$M_1(E) = \exp\left(-N_H \sigma_{el}(E)\right)$$

$$M_2(E) = A\,E^{-\gamma}$$

n = 8

p = 3

f = 5

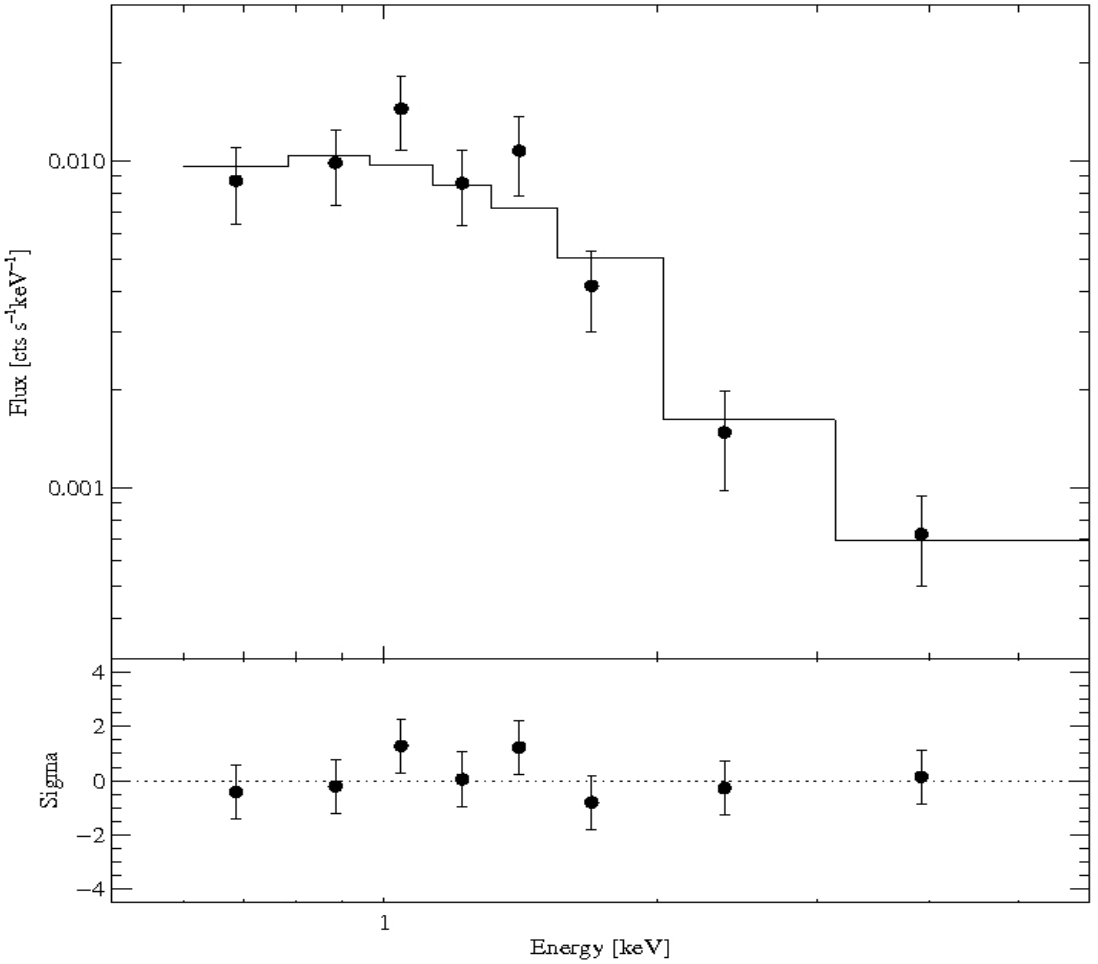

Chi square test:

What is the probability, that the date from the second set of measurements would deviate from the theoretical function more than do the set of measurements we already have in hands?

$y_i \pm \sigma_i$ ← **normal distribution with standard deviation**

So, this probability
is well calculated....

Chi square test:

What is the probability, that the date from the second set of measurements would deviate from the theoretical function more than do the set of measurements we already have in hands?

$y_i \pm \sigma_i$ ← **normal distribution with standard deviation**

So, this probability is well calculated....

$P(\chi^2) \subset 0.1 - 0.9$

$P(\chi^2) \sim 0.02$

$P(\chi^2) \sim 0.98$

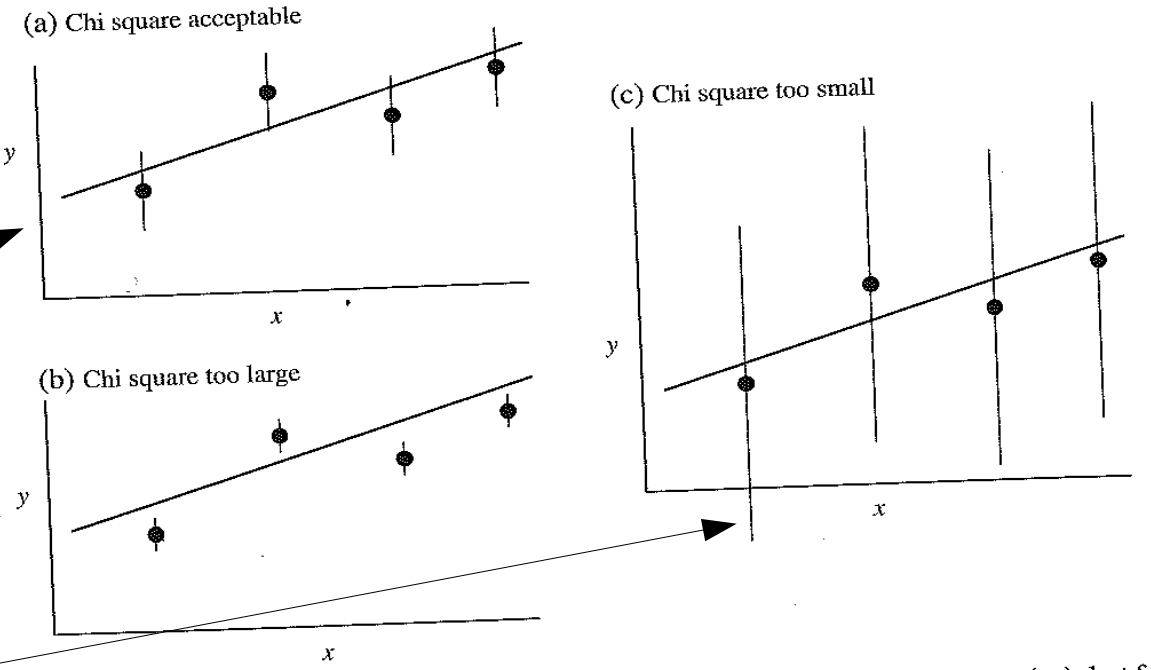

Figure 6.10. Results of chi square tests for different sizes of error bars (σ_i), but for the same data points x_i, y_i. (a) Moderate error bars. The chi square is acceptable because the average deviation is on the order of 1 standard deviation. (b) Small error bars. The deviations measured in units of σ_i are very large, leading to an unacceptably low χ^2 probability that fluctuations in another trial would exceed these. (c) Large error bars leading to an unacceptably high probability.

Chi square test:

Reduced chi square: $\chi^2_\nu \equiv \chi^2 / f$

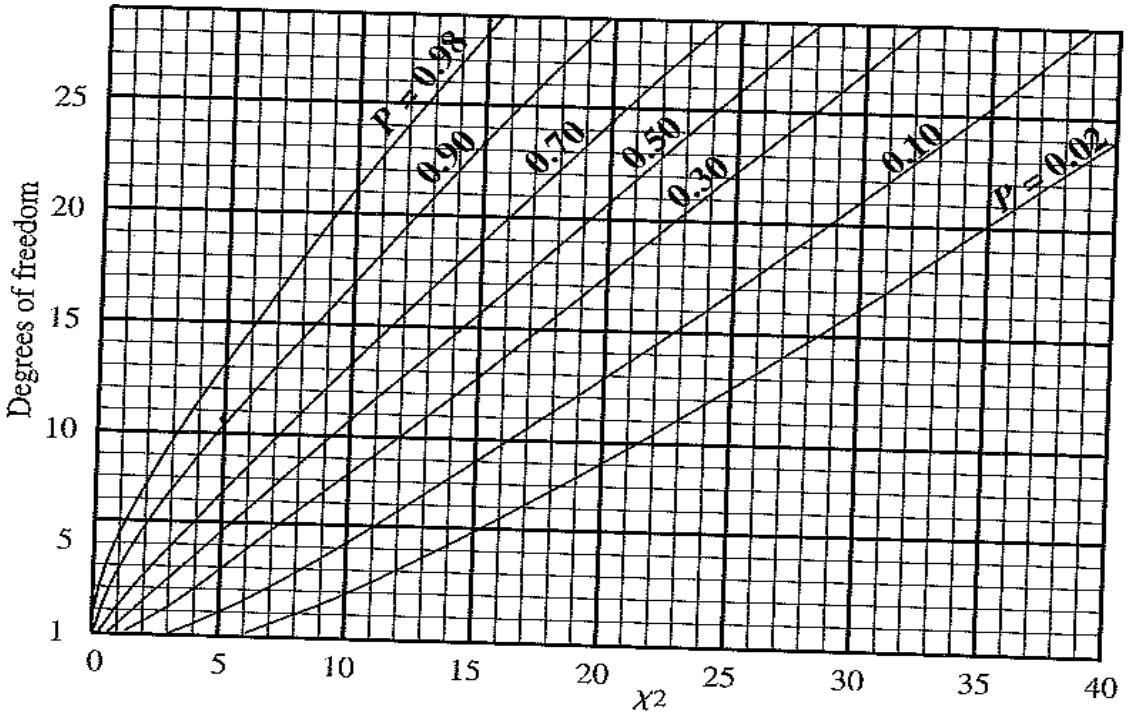

Figure 6.11. The probabilities P for the chi square test. The ordinate is the number of degrees of freedom (number of data points less number of variable parameters in trial function), and the abscissa is the value of χ^2. The curves give the probability that χ^2 would have a greater value in another set of measurements. [Adapted from Evans, *The Atomic Nucleus*, McGraw-Hill, 1955, p. 776, with permission.]

$P(\chi^2) \subset 0.1 - 0.9$

for $f = 10$

$0.49 < \chi^2_\nu < 1.6$

for $f = 200$

$0.87 < \chi^2_\nu < 1.13$

Homework: find A_{eff} (E), A_{eff} (off-axis angle), PSF for following gratings + mirrors + detector:

EINSTAIN, EXOSAT, ASCA, CHANDRA (LEG, HEG), XMM RGS, SUZAKU.

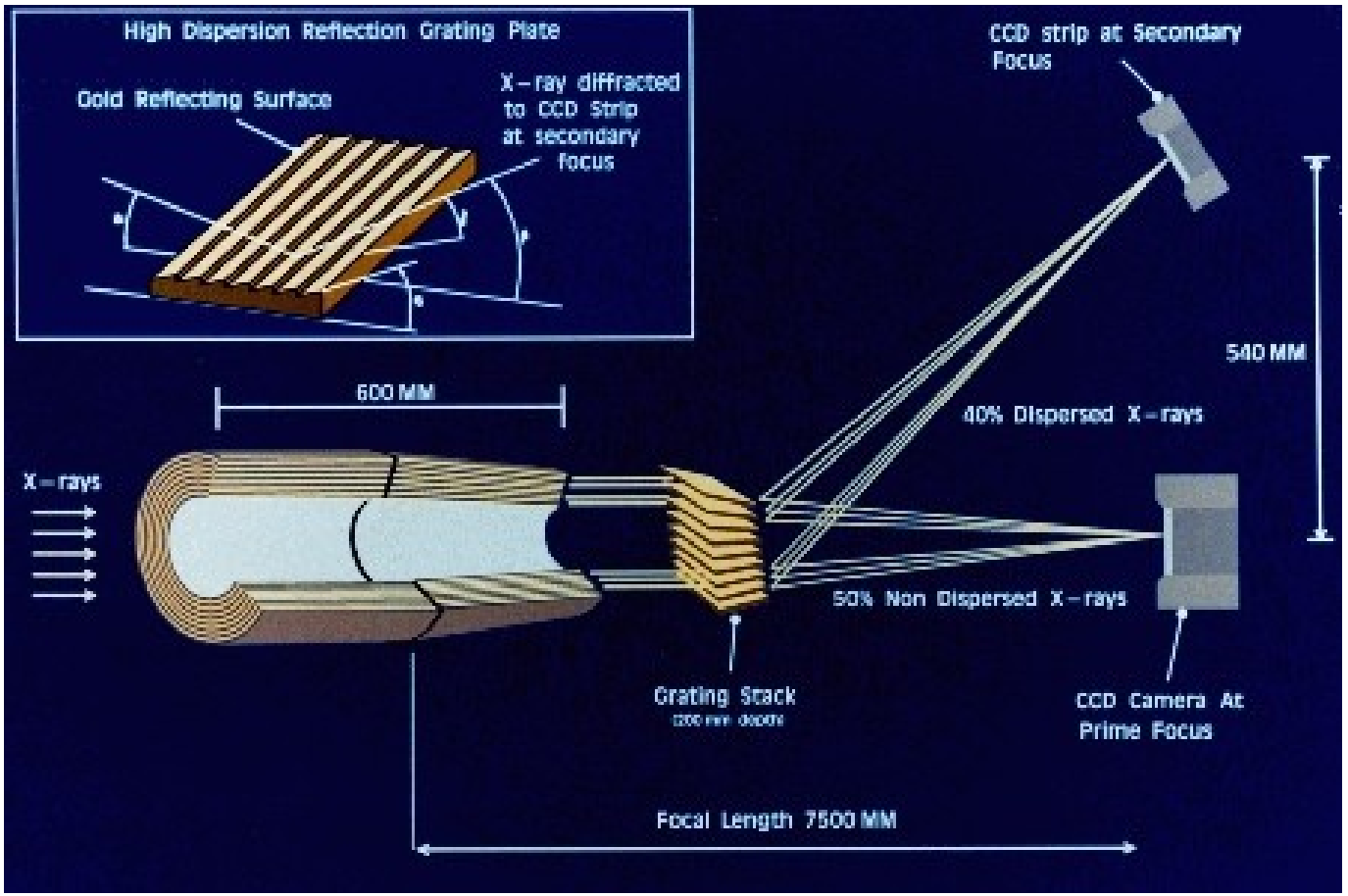

XMM-Newton

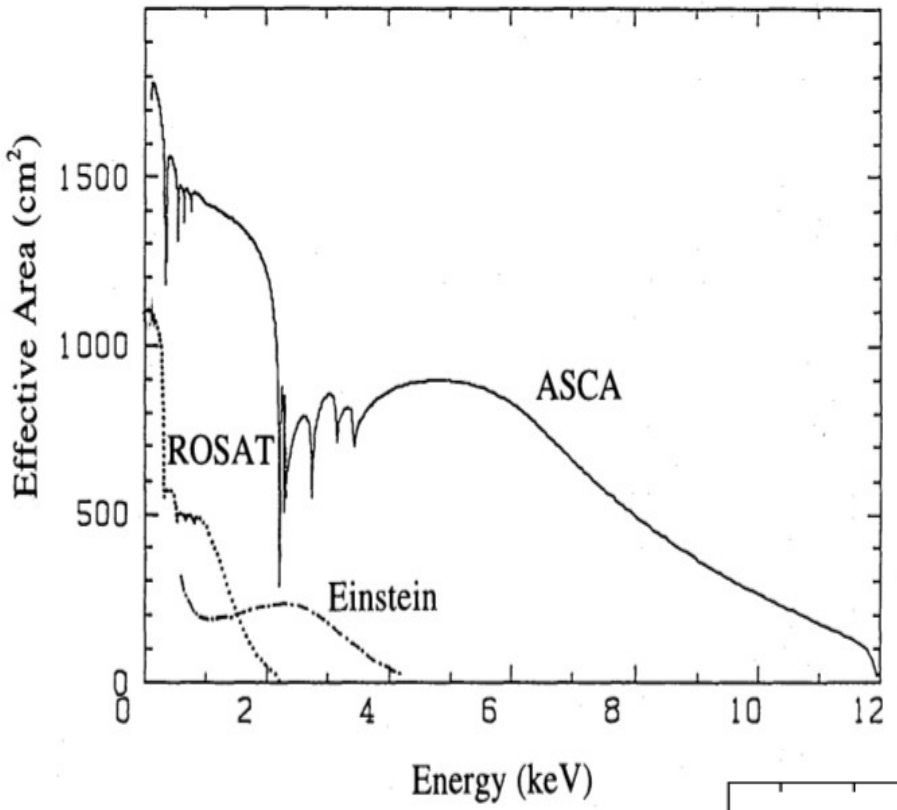
Effective Area (cm^2)
1500
1000
500
0
0
2
4
6
8
10
12
ROSAT
ASCA
Einstein
Energy (keV)

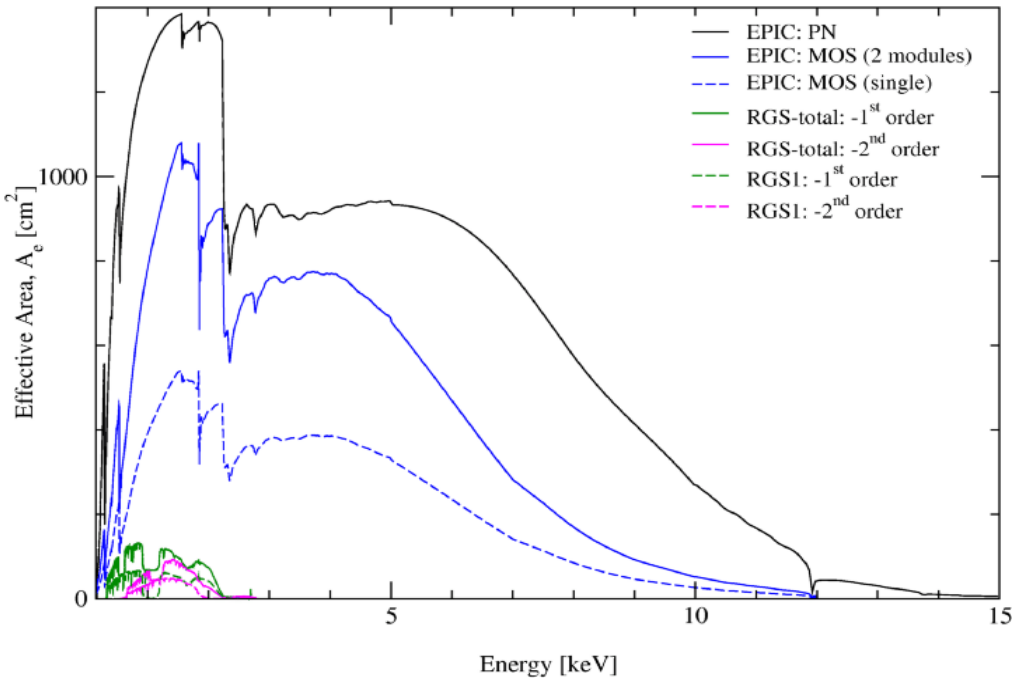
EPIC: PN
EPIC: MOS (2 modules)
EPIC: MOS (single)
RGS-total: -1st order
RGS-total: -2nd order
RGS1: -1st order
RGS1: -2nd order
Effective Area, A_e [cm^2]
1000
0
5
10
15
Energy [keV]

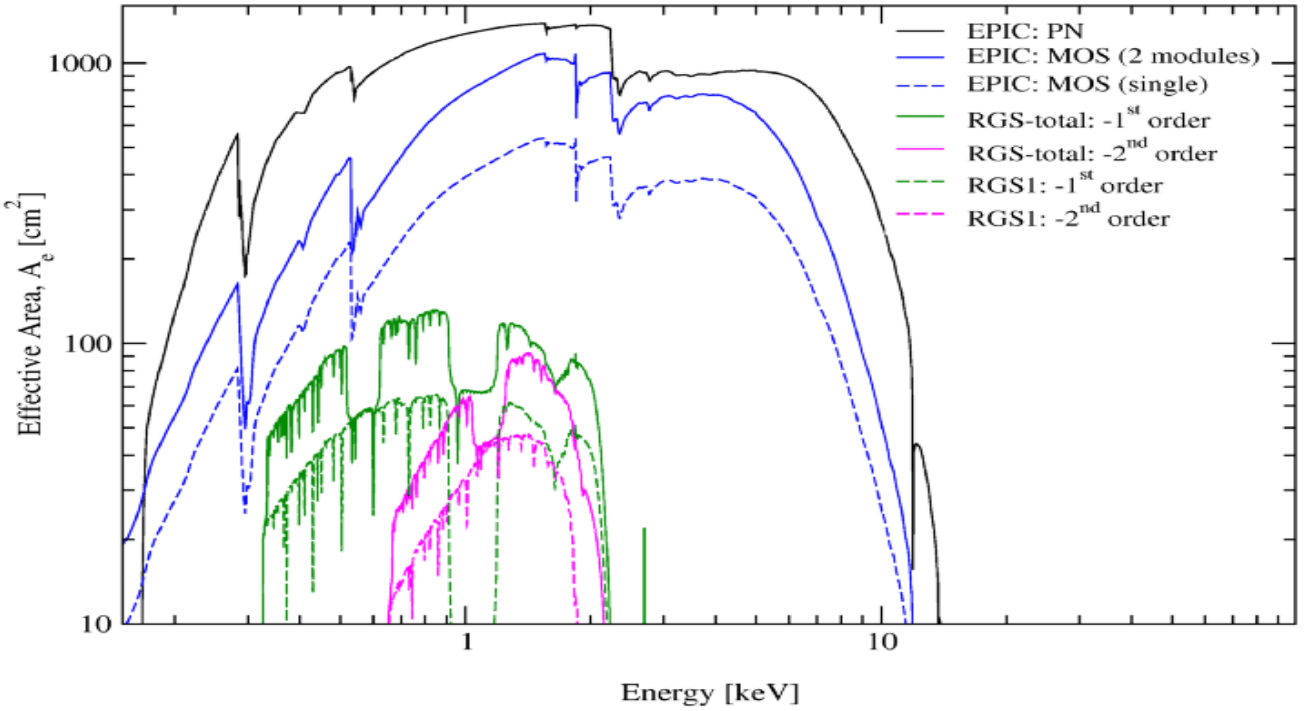
EPIC: PN
EPIC: MOS (2 modules)
EPIC: MOS (single)
RGS-total: -1st order
RGS-total: -2nd order
RGS1: -1st order
RGS1: -2nd order
Effective Area, A_e [cm^2]
1000
100
10
1
10
Energy [keV]

Hands – on sessions:

```
> ssh -X  libra
> exec tcsh
> source /work/agata/doktor_wyklad/init.csh
```

http://cxc.harvard.edu/ciao/

Principles of ranking the lecture:

- to be here

- to participate into discussions

- to make a homework

- hand – on sessions with the use of the computer.....

- exam – very simple :::)))

wi-fi password: a w sercu maj